Surface Tensions between Active Fluids and Solid Interfaces: Bare vs Dressed

R. Zakine,[1] Y. Zhao,[2,1] M. Knežević,[3] A. Daerr,[1] Y. Kafri,[4] J. Tailleur,[1] and F. van Wijland[1]
[1]Université Paris Diderot, Laboratoire Matière et Systèmes Complexes (MSC), UMR 7057 CNRS, F-75205 Paris, France
[2]School of Physics and Astronomy and Institute of Natural Sciences, Shanghai Jiao Tong University, Shanghai 200240, China
[3]Institut für Theoretische Physik, Technische Universität Berlin, Hardenbergstraße 36, D-10623 Berlin, Germany
[4]Department of Physics, Technion, Haifa 32000, Israel

(Received 2 October 2019; revised manuscript received 26 March 2020; accepted 7 May 2020; published 17 June 2020)

We analyze the surface tension exerted at the interface between an active fluid and a solid boundary in terms of tangential forces. Focusing on active systems known to possess an equation of state for the pressure, we show that interfacial forces are of a more complex nature. Using a number of macroscopic setups, we show that the surface tension is a combination of an equation-of-state abiding part and of setup-dependent contributions. The latter arise from generic setup-dependent steady currents which "dress" the measurement of the "bare" surface tension. The former shares interesting properties with its equilibrium counterpart, and can be used to generalize the Young-Laplace law to active systems. Finally, we show how a suitably designed probe can directly access this bare surface tension, which can also be computed using a generalized virial formula.

DOI: 10.1103/PhysRevLett.124.248003

Active particles are driven out of equilibrium through a dissipative exchange of energy and momentum with their environment, which endows them with anomalous thermomechanical properties [1–12]. Among these, the pressure exerted by active systems on their confining vessels has recently attracted a lot of interest [3–6,8,9,11,13–18]. In particular, the existence of an equation of state (EOS) for the pressure was established for a large subclass of these nonequilibrium and momentum-nonconserving systems. The defining feature which allows for an EOS is a self-propulsion force whose dynamics is independent of the positional and angular degrees of freedom [11]. This encompasses standard models such as run-and-tumble particles (RTPs), active Brownian particles (ABPs), and active Ornstein-Uhlenbeck particles (AOUPs), both non-interacting and in the presence of pairwise forces. For such systems, which are the focus of this Letter, macroscopic mechanical properties echo the equilibrium case with, for instance, equality of pressures in coexisting phases [13]. This raises the hope of a generalized thermodynamics [19–22].

While pressure is a state variable that controls bulk thermodynamics in equilibrium, interfacial properties rely on surface tension, perhaps the most elusive thermomechanical quantity whose microscopic origin has been the topic of long-standing debates [23–25]. Surface tension indeed controls a wealth of phenomena, from the demixing of binary mixtures to the wetting of surfaces, and the instability of thin films and jets [26–29]. Given the atypical properties of active matter at interfaces, from the accumulation at boundaries [30–32] to the wetting of soft gels by swarming bacteria [33–35], the study of surface tension in active systems has naturally attracted attention [7,36]. In particular, the surface tension of active particles at a liquid-gas interface in a system undergoing motility-induced phase separation has been measured using an expression derived for Hamiltonian systems [37,38]. Despite stable interfaces, this liquid-gas surface tension was, somewhat surprisingly, found to be negative [7,12,22]. Its thermodynamic role has nevertheless been confirmed: it controls the pressure drop through the boundary of a circular droplet of radius R through a Laplace pressure $\Delta P = \gamma/R$ [22]. This combination of surprising and familiar aspects of interfacial physics enjoins us to clarify the microscopic origin of surface tension in active systems and in particular its mechanical implications, which have been little discussed so far. Accounting for capillary and wetting phenomena in active matter is a formidable program which we attack by elucidating the interfacial properties of active fluids in contact with a solid boundary. For simplicity, we work in two dimensions throughout the Letter, the generalization to higher dimensions being straightforward.

In the absence of an established thermodynamic route, it is natural to revert to mechanics. The Langmuir balance [39] is a standard tool to measure the tangential force exerted on an interface between a fluid and a solid in equilibrium, and hence to access surface tension. Take a mobile wall made of two different materials confining a fluid in a cavity [see Fig. 1(a)]. Moving the wall changes the contact area between the fluid and each material. In equilibrium, the corresponding tangential force exerted by the fluid on the wall is thus given by the difference of surface tensions between the fluid and each material $\Delta\gamma = \gamma_2 - \gamma_1$. This highlights an important property of

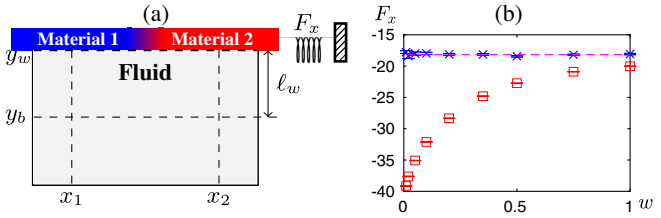

FIG. 1. (a) Modified Langmuir setup: The mobile upper boundary, made of two different materials, is modeled by a potential $V_w(x,y) = \lambda(x)(y-y_w)^4$ for $y > y_w$. The function $\lambda(x) = \lambda_1 + [(\lambda_2 - \lambda_1)/2]\{1 + \tanh[(x-\ell)/w)]\}$ interpolates smoothly between the two material stiffnesses λ_1 and λ_2. (b) Tangential force F_x, measured from Eq. (2), exerted on the upper wall vs the width w of the junction. In equilibrium (crosses), F_x is independent of w and given by $\Delta\gamma$, Eq. (3) (dashed line). By contrast, for the active system (squares), F_x depends on w. Parameters: $\lambda_1 = 5$, $\lambda_2 = 0.05$, $\ell = L_x/2$. Equilibrium Brownian simulations: $D = 8.2$, $L_x = 2L_y = 80$. ABPs: $v_0 = 5$, $\tau = 1$, $L_x = 2L_y = 1280$, $\ell_w = 10$. See Ref. [40] for numerical details and for similar results using alternative choices of V_w, as well as RTPs and AOUPs. Throughout, the bulk density is 1.

equilibrium systems: the tangential force is independent of the details of the junction between the two materials.

Strikingly, in this Letter, we show that self-propelled particles such as ABPs, RTPs, or AOUPs exhibit a very different physics: already at the noninteracting level, but also in the presence of pairwise forces, the tangential force now strongly depends on the details of the junction between the two materials.

We indeed show that, in addition to an intrinsic, *bare*, EOS-abiding contribution $\Delta\gamma$, the emergence of junction-dependent currents leads to an extra contribution for the tangential force, whence preventing the existence of an EOS. The Langmuir setup of Fig. 1 hence only accesses a surface tension that we refer to as *dressed* by these junction-dependent currents [47]: the reading of the surface tension depends on the probe used for its measurement. We show that, in addition to its intrinsic, junction-independent nature, the bare surface tension plays a versatile role in other surface phenomena, much like in equilibrium. For example, we establish how it controls the Young-Laplace corrections to the normal pressure felt by a circular confining cavity. We then suggest a second setting designed to make the contribution of the currents vanish, hence providing a direct mechanical measurement of the bare surface tension. Finally, a lot of effort has been invested in the past to derive the pressure of active fluids using a virial approach [4,5,15,18,48]. Here we introduce a different virial, which offers a macroscopic route to the bare surface tension.

Current-induced tangential forces.—To model the experiment depicted in Fig. 1(a), we follow Ref. [49] and disregard the internal dynamics of the wall, which we model as a confining potential $V_w(x,y)$. We consider the dynamics of N noninteracting active particles:

$$\dot{\mathbf{r}}_i = v_0\mathbf{u}_i - \mu\nabla_{\mathbf{r}_i}V_w(\mathbf{r}_i), \tag{1}$$

with μ the particle's mobility, $v_0\mathbf{u}_i/\mu$ the active force on particle i, and $\mathbf{u}_i = (\cos\theta_i, \sin\theta_i)$ its orientation. To focus on the new features due to activity, we consider the simplest case of RTPs and ABPs and denote by τ their persistence time. The generalization to AOUPs and pairwise forces is detailed in Ref. [40]. The tangential force exerted by the particles on the upper wall is given by

$$F_x = \int_{x_1}^{x_2} dx \int_{y_b}^{\infty} dy \rho(x,y)\partial_x V_w(x,y) \tag{2}$$

where ρ is the mean density of particles, x_1 and x_2 are abscissa far away from the junction between the two materials, and y_b is an ordinate in the "bulk" of the system, at a distance $\ell_w \equiv y_w - y_b$ from the upper confining wall (see Fig. 1). For an equilibrium ideal gas, a direct computation leads to

$$F_x = \gamma_2 - \gamma_1 \quad \text{with} \quad \gamma_k \equiv -\int_{y_w}^{\infty} dy kT\rho(x_k,y). \tag{3}$$

As illustrated in Fig. 1(b), F_x is independent of the details of the junction between the two walls. This is expected from thermodynamical considerations, from which the EOS Eq. (3) can be derived [50].

For ABPs, on the contrary, Fig. 1(b) shows that F_x has a strong dependence on the width of the junction w. To elucidate this fact analytically, we introduce the average density field $\rho(\mathbf{r}) = \langle\sum_i \delta(\mathbf{r}-\mathbf{r}_i)\rangle$, where the brackets represent averages over the active-force statistics. It evolves according to the continuity equation

$$\partial_t\rho = -\boldsymbol{\nabla}\cdot\mathbf{J}, \qquad \mathbf{J} = v_0\mathbf{m} - \rho\mu\boldsymbol{\nabla}V_w \tag{4}$$

where the local orientation field $\mathbf{m}(\mathbf{r}) = \langle\sum_i \mathbf{u}_i\delta(\mathbf{r}-\mathbf{r}_i)\rangle$ controls the contribution of self-propulsion to the particle flow. In the steady state (see, e.g., Ref. [6])

$$m_\alpha = -\partial_\beta\left[v_0\tau\left(Q_{\alpha\beta} + \frac{\rho\delta_{\alpha\beta}}{2}\right) - \mu\tau m_\alpha\partial_\beta V_w\right] \tag{5}$$

where Q measures the local nematic order through $Q_{\alpha\beta}(\mathbf{r}) = \langle\sum_i(u_{i,\alpha}u_{i,\beta} - \delta_{\alpha\beta}/2)\delta(\mathbf{r}-\mathbf{r}_i)\rangle$, with Greek letters referring to space directions. From Eqs. (2) and (4), the tangential force F_x exerted on the upper wall can be written as

$$F_x = F_D + \int_{x_1}^{x_2}\int_{y_b}^{\infty}\frac{v_0}{\mu}m_x(x,y)dxdy \tag{6}$$

where F_D is the total drag experienced by particles around the junction:

$$F_D = -\frac{1}{\mu}\int_{x_1}^{x_2} dx \int_{y_b}^{\infty} dy J_x = -\mu^{-1} \sum_{x_i \in [x_1,x_2]; y_i > y_b} \langle \dot{\mathbf{r}}_i \cdot \mathbf{e}_x \rangle. \tag{7}$$

Equation (6) has an appealing physical interpretation in terms of force balance: the total active force exerted by the particles, which is the second term on the rhs of Eq. (6), is split between the force exerted on the upper wall F_x and the friction force exerted on the environment, $-F_D$. Using Eq. (5), the isotropy of the bulk, translational invariance far from the junction, and that $\int_{y_b}^{\infty} dy Q_{xx}(x,y) = 0$ for $x = x_1$ or $x = x_2$ [40], the force balance Eq. (6) can be rewritten as

$$F_x = F_D + \gamma_2 - \gamma_1 \tag{8}$$

where we define the bare surface tension γ_k as

$$\gamma_k = -\frac{v_0^2 \tau}{2\mu}\left(\int_{y_b}^{\infty} dy \rho(x_k, y) - \int_{y_b}^{y_w} dy \rho_0\right). \tag{9}$$

Note that the final integral in Eq. (9) cancels out in Eq. (8); it ensures that γ_k does not depend on y_b. Equations (8) and (9) form a central result of this Letter; They are exact in the macroscopic limit $L_x, L_y, \ell_w \to \infty$ with $\rho_0 = N/L^2$ finite and $\ell_p \ll \ell_w \ll L_x, L_y$, where $\ell_p = v_0\tau$ is the persistence length. The result has several implications. As in equilibrium, $\Delta\gamma = \gamma_2 - \gamma_1$ is a contribution to F_x that is independent of the details of the junction; Eq. (9) is the EOS for γ_k. It is determined by the excess density accumulated at the wall compared to the bulk values. Note that γ_k can be measured independently in a translationally invariant system and thus solely depends on the interaction between the active fluid and wall k. Conversely, F_D strongly depends on the details of the junction: the presence of an asymmetric potential combined with the nonequilibrium dynamics of the active particles generates, as in a ratchet, steady currents which are bound to be junction dependent; the latter give rise to a nonzero drag which dresses F_x. Figure 2(a) indeed shows that the dependence of F_x on the width w of the junction is entirely due to the variations of F_D, whereas $\Delta\gamma$ is independent of w, and can be obtained from independent measurements of $\gamma_{1,2}$. Figure 2(b) suggests that the junction generates a current field which decays slowly with the distance to the junction. This is consistent with recent results on the power-law decay of currents generated by asymmetric obstacles located in the bulk of active fluids [52,53]. Note that the macroscopic limit defined above, in which $\ell_w \ll L_x, L_y$ ensures that $\Delta\gamma$ is indeed independent of the junction. Otherwise, if $\ell_w \sim L_x, L_y$, the measurement of $\Delta\gamma$ itself could be modified by the currents. In our numerics, we found that $\ell_w = 2\ell_p$ was sufficient for the system to be isotropic at $y = y_b$ and gives a reliable measurement of the bare $\Delta\gamma$.

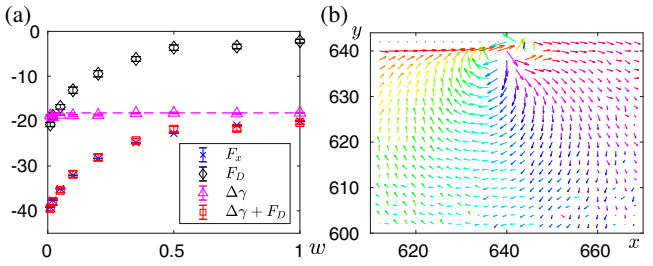

FIG. 2. (a) Comparison between F_x and the sum of the bare $\Delta\gamma$ and the junction-dependent drag F_D, measured from Eq. (7). $\Delta\gamma$ coincides with its independent measurements using Eq. (9) in homogeneous systems bounded by upper potentials $V_1 = V_w(x \ll l)$ and $V_2 = V_w(x \gg l)$ (dashed line). (b) Map of the current around the junction for $|\mathbf{J}| > 10^{-6}$. The length of each vector is proportional to $\log|\mathbf{J}/10^{-6}|$; the color encodes their directions. Parameters: $\lambda_1 = 5$, $\lambda_2 = 0.05$, $l = L_x/2$, $v = 5$, $\tau = 1$, $L_x = 2L_y = 1280$. For the current field, $w = 0.01$.

As expected, in the $\tau \to 0$ limit, with $v_0^2\tau$ fixed, active particles behave as equilibrium colloids at an effective temperature $kT_{\text{eff}} = v_0^2\tau/(2\mu)$ and Eq. (9) reduces to its equilibrium counterpart Eq. (3). The partial cancellation of the two integrals in Eq. (9) then stems from the fact that, unlike active particles, passive ones have a steady-state distribution which is a local function of the external potential $V_w(x,y)$. In this limit, as for true equilibrium systems, no currents survive in the steady state; F_D vanishes and F_x is then a direct measurement of the bare, EOS-abiding contribution $\Delta\gamma$.

Finally, the existence of an EOS for surface tension extends to equilibrium fluids with interactions. Similarly, all our derivations extend to active fluids with pairwise forces at the cost of a lengthier expression for γ [40].

Bare surface tension and Laplace pressure corrections.—The use of surface tension is not limited, in equilibrium, to the measurement of tangential forces. A famous example is that of the Young-Laplace law which shows how surface tension impacts the pressure on a circular interface. In our solid-liquid framework, this amounts to computing the normal pressure exerted by an active fluid on a circular confining wall of radius R. The pressure is known to admit finite-size corrections that decay as $1/R$ [3,8,54], in a manner reminiscent of the equilibrium Laplace pressure corrections. To explicitly connect these corrections to our bare surface tension, we compute the pressure from $2\pi R P(R) = \int \rho(r)\partial_r V_w r dr d\theta$. In the flux-free steady state observed in such a system, one has $\mu\rho(r)\partial_r V_w = v_0 m_r$. Using Eq. (5) in circular coordinates then leads to

$$P(R) = -\frac{v_0}{\mu R}\int_0^{\infty} \partial_r\left[v_0\tau\left(Q_{rr} + \frac{\rho}{2}\right) - \mu\tau m_r \partial_r V_w\right] r dr$$
$$-\frac{v_0}{\mu R}\int_0^{\infty} [v_0\tau(Q_{rr} - Q_{\theta\theta}) - \mu\tau m_r \partial_r V_w] dr.$$

Integrating by parts the first term on the rhs leads to $P(R) = \mu^{-1}R^{-1}\int_0^\infty v_0^2\tau(Q_{\theta\theta} + \rho/2)dr$. Adding and subtracting the bulk pressure $P_b = \rho_0 v_0^2\tau/(2\mu)$ then leads, in the large R limit, to

$$P(R) \simeq P_b - \frac{1}{R}\left[\int_0^R \frac{v_0^2\tau\rho_0}{2\mu}dr - \int_0^\infty \frac{v_0^2\tau\rho(r)}{2\mu}dr\right] \quad (10)$$

where ρ_0 is the density at $r = 0$. Importantly, Eq. (10) shows that the pressure can be written as a generalized Young-Laplace law $P(R) = P_b - \gamma/R + o(1/R)$, with γ identified as the bare surface tension defined in Eq. (9), a connection not made previously. Despite its dressing by currents in the microscopic setting of Fig. 1, the bare surface tension thus plays an important role in active fluids. We now tackle the question of its direct mechanical measurement.

Direct measurement of the bare surface tension.—The currents arising in the Langmuir setup, which prevents the direct measurement of the bare surface tension, are due to the junction. Furthermore, the Langmuir setup only gives access to the difference between the two fluid-solid surface tensions $\Delta\gamma$. We now consider instead the setup depicted in Fig. 3, in which, as we show below, the force exerted by the active fluid on a piston allows one to directly access the (bare) surface tension between the fluid and the walls of the container. The latter are modeled by a confining potential V_w while the piston is modeled by a confining potential $V_p(x) = \lambda_p(x-x_p)^4\Theta(x-x_p)$. (See Ref. [40] for details.) Using Eq. (1), the total force $F_x = \int_{x_b}^\infty dx\int_{-\infty}^\infty dy\rho(x,y)\partial_x V_p(x,y)$ exerted on the piston can be rewritten as

$$F_x = -\frac{1}{\mu}\left\langle \sum_{i|x_i>x_b} \dot{x}_i \right\rangle + \int_{x_b}^\infty dx\int_{-\infty}^\infty dy\frac{v_0}{\mu}m_x \quad (11)$$

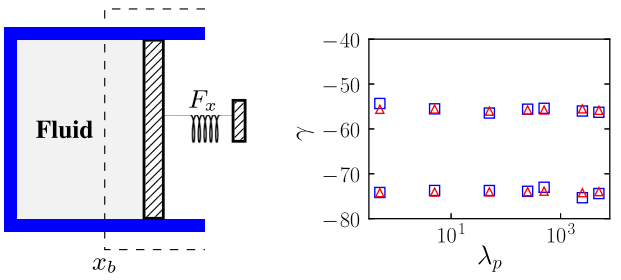

FIG. 3. Left: Setup used to directly measure the bare surface tension. Right: The measurement of γ for two different confining materials is independent of the piston's stiffnesses λ_p. Measuring γ from the force on the piston (squares) or from Eq. (9) evaluated at $x = x_b$ (triangles) leads to consistent results. Parameters: $L_x = L_y = 50$, $v_0 = 5$, $\tau = 1$. Upper and lower results correspond to confining materials of stiffness $\lambda = 5$ and $\lambda = 0.05$, respectively. The distance between the two measurements corresponds to $\Delta\gamma$ in Fig. 2(a).

Equation (5) then allows us to simplify Eq. (11) into

$$F_x = F_D + \int_{-\infty}^\infty dy\rho(x_b,y)\frac{v_0^2\tau}{2\mu} \quad (12)$$

where F_D is defined as the first term on the rhs of Eq. (11) and we have used that all fields vanish at infinity and that $\int_{-\infty}^\infty Q_{xx}(x_b,y)dy = 0$ [40]. Introducing the bulk pressure $P_b = \rho_0 v_0^2\tau/(2\mu)$, F_x is finally given by

$$F_x = F_D + P_b L_y - 2\gamma \quad (13)$$

with γ defined as in Eq (9), assuming for simplicity that the upper and lower walls are identical. At first glance, Eq. (13) seems to imply that, once again, the bare surface tension is dressed by currents through the drag F_D. Note, however, that the average density of particles in the half-plane defined by $x > x^*$ is constant, for all x^*, in the steady state. Since $\dot{\rho} = -\nabla\cdot\mathbf{J}$, this implies that $\int_{-\infty}^\infty J_x(x^*,y)dy = 0$. Integrating this from $x^* = x_b$ up to infinity shows that $F_D = 0$ in this setup: F_x thus provides a direct measurement of the bare surface tension between the fluid and the upper and lower walls, as shown in Fig. 3 (right).

A virial route to surface tension.—In equilibrium, the mechanical route to surface tension can be circumvented by free energy considerations, a path which is not accessible to active systems. Another historical route to EOS was proposed by Clausius through the virial. This has recently been applied successfully to determine the pressure of active fluids when an EOS exists [4,5,15,18,48]. We now extend this approach to surface tension.

We consider N active particles in a box of dimensions $L_x \times L_y$, evolving according to

$$\dot{\mathbf{r}}_i = v_0\mathbf{u}_i + \mu\mathbf{F}_i^{\text{ext}} + \sum_j \mu\mathbf{F}_{j\to i} \quad (14)$$

where $\mathbf{F}_i^{\text{ext}}$ is the force exerted by the walls to confine particle i. Up to now, we had for clarity considered noninteracting particles. Our results however extend to particles interacting via pairwise forces $\mathbf{F}_{j\to i} \equiv -\nabla\Phi(\mathbf{r}_i - \mathbf{r}_j)$, a case that we now consider more explicitly. To develop a virial approach to surface tension, we introduce a modified virial $\mathcal{V}(t) \equiv \frac{1}{2}\sum_i\langle\mathbf{r}_i(t)\cdot\mathbf{r}_i^*(t)\rangle$, where $\mathbf{r}_i^* = (x_i, -y_i)$ are divergence-free vectors. We now use that $\dot{\mathcal{V}}(t) = 0$ in the steady state to get

$$0 = v_0\sum_i\langle\mathbf{u}_i\cdot\mathbf{r}_i^*\rangle + \mu\left\langle\sum_i\mathbf{F}_i^{\text{ext}}\cdot\mathbf{r}_i^*\right\rangle + \mu\left\langle\sum_{ij}\mathbf{F}_{j\to i}\cdot\mathbf{r}_i^*\right\rangle. \quad (15)$$

In the limit of hard walls, the external force density along a side of the box is naturally decomposed into pressure and surface tension contributions, as depicted in Fig. 4. Using this

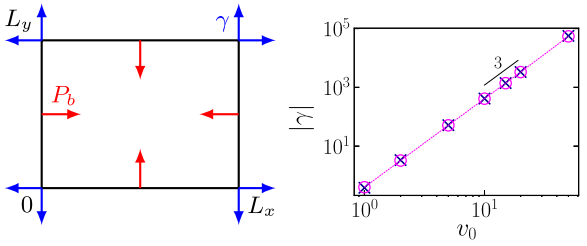

FIG. 4. Left: For hard walls, $\mathbf{F}_i^{\text{ext}}$ can be decomposed into pressure (red) and surface tension (blue). Right: Surface tension on a hard wall as a function of v_0. The virial Eq. (18) (circles) coincides with Eq. (9) (crosses). A fit of the data to Eq. (19) leads to $c \simeq 0.40 \pm 0.02$ for ABPs. Parameters: $L_x = 2L_y = 120$, $\mu = 1$, $\tau = 1$, $\lambda = 10^4$.

decomposition, a direct evaluation shows that $\langle \sum_i \mathbf{F}_i^{\text{ext}} \cdot \mathbf{r}_i^* \rangle = \gamma L_x + \gamma(L_x - L_y) - \gamma L_y + P_b L_x L_y - P_b L_y L_x$. The pressure contribution cancels out, since $\mathbf{r}^*$ is divergenceless, and Eq. (15) leads to our modified virial for the surface tension:

$$\gamma = -\frac{1}{2(L_x - L_y)} \sum_i \left\langle \mathbf{r}_i^* \cdot \left(\frac{v_0}{\mu} \mathbf{u}_i + \sum_j \mathbf{F}_{j \to i} \right) \right\rangle. \tag{16}$$

Much like the usual virial formula, the presence of $\mathbf{r}_i^*$ in Eq. (16) makes its numerical measurement difficult [15]. Using that $\partial_t \langle \mathbf{u}_i \cdot \mathbf{r}_i^* \rangle = 0$ in the steady state, we arrive at

$$\langle \mathbf{u}_i \cdot \mathbf{r}_i^* \rangle = \tau \mu \langle \mathbf{F}_i^{\text{ext}} \cdot \mathbf{u}_i^* \rangle + \tau \sum_j \mu \langle \mathbf{F}_{j \to i} \cdot \mathbf{u}_i^* \rangle, \tag{17}$$

where we have used $\langle \mathbf{u}_i \cdot \mathbf{u}_i^* \rangle = 0$ in the steady state, with $\mathbf{u}_i^* = (\cos\theta_i, -\sin\theta_i)$. All in all, the surface tension can thus be written in a numerically friendly way as

$$\gamma = -\frac{1}{2(L_x - L_y)} \left[v_0 \tau \left(\sum_i \langle \mathbf{F}_i^{\text{ext}} \cdot \mathbf{u}_i^* \rangle + \sum_{ij} \langle \mathbf{F}_{j \to i} \cdot \mathbf{u}_i^* \rangle \right) + \frac{1}{2} \sum_{ij} \langle \mathbf{F}_{j \to i} \cdot (\mathbf{r}_i^* - \mathbf{r}_j^*) \rangle \right]. \tag{18}$$

Equation (16) of course also holds for a passive dynamics in which it offers an alternative to the Kirkwood-Buff formula [37], of which Eq. (18) is a generalization to active systems for a solid-liquid interface. In the noninteracting limit, dimensional analysis shows the surface tension between an active gas and a hard wall to be given by

$$\gamma = -c \frac{v_0^3 \tau^2}{\mu} \rho_0, \tag{19}$$

where c is a dimensionless constant. Figure 4 confirms the scaling Eq. (19), as well as the agreement between Eqs. (9) and (18), generalized in Ref. [40] for pairwise forces.

Conclusion.—The tangential forces exerted on an interface result from a bare, EOS-abiding contribution and a drag resulting from a setup-dependent current, a signature of the nonequilibrium nature of active particles. Our results cover active matter systems whose pressure admits an EOS. Yet, current-induced drags will extend beyond this class, for instance in the presence of aligning interactions, and they will similarly enter the mechanical balance controlling tangential forces. The fate of the bare surface tension, however, is a challenging open question. The models we consider fall into the class of dry active matter, where vibrated disks of varying anisotropies offer an interesting test bench [9,55]. Since we study interfacial phenomena, where momentum is lost to the solid surface, the presence of a surrounding fluid is expected to play a less fundamental role than it does for the pressure by restoring a local conservation law for the momentum field in the bulk of the system. On the contrary, the existence of an EOS for the total pressure of wet systems makes active suspensions interesting candidates to probe our results.

F. v W., J. T., and R. Z. thank K. Mandadapu at UC Berkeley for hospitality and discussions, J. T. acknowledges support from ANR Bactterns, Y. K. acknowledges support from I-CORE Program of the Planning and Budgeting Committee of the Israel Science Foundation, from an Israel Science Foundation grant and from the NSF-BSF. J. T. and Y. K. acknowledge support from a joint CNRS-MOST grant. M. K. acknowledges support from the Alexander von Humboldt Foundation.

R. Z. and Y. Z. contributed equally to this work.

[1] R. Di Leonardo, L. Angelani, D. Dell'Arciprete, G. Ruocco, V. Iebba, S. Schippa, M. Conte, F. Mecarini, F. De Angelis, and E. Di Fabrizio, Proc. Natl. Acad. Sci. U.S.A. **107**, 9541 (2010).
[2] A. Sokolov, M. M. Apodaca, B. A. Grzybowski, and I. S. Aranson, Proc. Natl. Acad. Sci. U.S.A. **107**, 969 (2010).
[3] S. A. Mallory, A. Šarić, C. Valeriani, and A. Cacciuto, Phys. Rev. E **89**, 052303 (2014).
[4] S. C. Takatori, W. Yan, and J. F. Brady, Phys. Rev. Lett. **113**, 028103 (2014).
[5] X. Yang, M. L. Manning, and M. C. Marchetti, Soft Matter **10**, 6477 (2014).
[6] A. P. Solon, Y. Fily, A. Baskaran, M. E. Cates, Y. Kafri, M. Kardar, and J. Tailleur, Nat. Phys. **11**, 673 (2015).
[7] J. Bialké, J. T. Siebert, H. Löwen, and T. Speck, Phys. Rev. Lett. **115**, 098301 (2015).
[8] C. Sandford, A. Y. Grosberg, and J.-F. Joanny, Phys. Rev. E **96**, 052605 (2017).
[9] G. Junot, G. Briand, R. Ledesma-Alonso, and O. Dauchot, Phys. Rev. Lett. **119**, 028002 (2017).
[10] G. Vizsnyiczai, G. Frangipane, C. Maggi, F. Saglimbeni, S. Bianchi, and R. Di Leonardo, Nat. Commun. **8**, 15974 (2017).

[11] Y. Fily, Y. Kafri, A. P. Solon, J. Tailleur, and A. Turner, J. Phys. A **51**, 044003 (2017).
[12] A. Patch, D. M. Sussman, D. Yllanes, and M. C. Marchetti, Soft Matter **14**, 7435 (2018).
[13] A. P. Solon, J. Stenhammar, R. Wittkowski, M. Kardar, Y. Kafri, M. E. Cates, and J. Tailleur, Phys. Rev. Lett. **114**, 198301 (2015).
[14] N. Nikola, A. P. Solon, Y. Kafri, M. Kardar, J. Tailleur, and R. Voituriez, Phys. Rev. Lett. **117**, 098001 (2016).
[15] T. Speck and R. L. Jack, Phys. Rev. E **93**, 062605 (2016).
[16] U. Marini Bettolo Marconi, C. Maggi, and S. Melchionna, Soft Matter **12**, 5727 (2016).
[17] F. Ginot, A. Solon, Y. Kafri, C. Ybert, J. Tailleur, and C. Cottin-Bizonne, New J. Phys. **20**, 115001 (2018).
[18] G. Falasco, F. Baldovin, K. Kroy, and M. Baiesi, New J. Phys. **18**, 093043 (2016).
[19] F. Ginot, I. Theurkauff, D. Levis, C. Ybert, L. Bocquet, L. Berthier, and C. Cottin-Bizonne, Phys. Rev. X **5**, 011004 (2015).
[20] A. P. Solon, J. Stenhammar, M. E. Cates, Y. Kafri, and J. Tailleur, Phys. Rev. E **97**, 020602(R) (2018).
[21] J. Rodenburg, M. Dijkstra, and R. van Roij, Soft Matter **13**, 8957 (2017).
[22] A. P. Solon, J. Stenhammar, M. E. Cates, Y. Kafri, and J. Tailleur, New J. Phys. **20**, 075001 (2018).
[23] M. V. Berry, Phys. Educ. **6**, 79 (1971).
[24] A. Marchand, J. H. Weijs, J. H. Snoeijer, and B. Andreotti, Am. J. Phys. **79**, 999 (2011).
[25] J. Rowlinson and B. Widom, *Molecular Theory of Capillarity* (Clarendon, Oxford, 1982), Vol. 56.
[26] P.-G. De Gennes, F. Brochard-Wyart, and D. Quéré, *Capillarity and Wetting Phenomena: Drops, Bubbles, Pearls, Waves* (Springer Science & Business Media, New York, 2013).
[27] D. Bonn, J. Eggers, J. Indekeu, J. Meunier, and E. Rolley, Rev. Mod. Phys. **81**, 739 (2009).
[28] J. Eggers and E. Villermaux, Rep. Prog. Phys. **71**, 036601 (2008).
[29] R. V. Craster and O. K. Matar, Rev. Mod. Phys. **81**, 1131 (2009).
[30] J. Elgeti and G. Gompper, Europhys. Lett. **85**, 38002 (2009).
[31] J. Tailleur and M. Cates, Europhys. Lett. **86**, 60002 (2009).
[32] J. Elgeti and G. Gompper, Europhys. Lett. **101**, 48003 (2013).
[33] D. B. Kearns, Nat. Rev. Microbiol. **8**, 634 (2010).
[34] N. C. Darnton, L. Turner, S. Rojevsky, and H. C. Berg, Biophys. J. **98**, 2082 (2010).
[35] M. Hennes, J. Tailleur, G. Charron, and A. Daerr, Proc. Natl. Acad. Sci. U.S.A. **114**, 5958 (2017).
[36] S. Paliwal, V. Prymidis, L. Filion, and M. Dijkstra, J. Chem. Phys. **147**, 084902 (2017).
[37] J. G. Kirkwood and F. P. Buff, J. Chem. Phys. **17**, 338 (1949).
[38] F. P. Buff, J. Chem. Phys. **23**, 419 (1955).
[39] I. Langmuir, J. Am. Chem. Soc. **39**, 1848 (1917).
[40] See Supplemental Material at http://link.aps.org/supplemental/10.1103/PhysRevLett.124.248003, which includes theoretical and numerical details, as well as Refs. [22,41–46].
[41] P. Jung and P. Hänggi, Phys. Rev. A **35**, 4464 (1987).
[42] C. Van den Broeck and P. Hänggi, Phys. Rev. A **30**, 2730 (1984).
[43] G. Szamel, Phys. Rev. E **90**, 012111 (2014).
[44] M. E. Cates and J. Tailleur, Europhys. Lett. **101**, 20010 (2013).
[45] A. P. Solon, M. Cates, and J. Tailleur, Eur. Phys. J. Special Topics **224**, 1231 (2015).
[46] N. G. Van Kampen, *Stochastic Processes in Physics and Chemistry* (Elsevier, 1992), Vol. 1.
[47] Nonequilibrium fluctuations prevent the direct measurement of the bare surface tension through the generation of currents. We use the word *dressed* by analogy to quantum fluctuations that dress classical observables.
[48] R. G. Winkler, A. Wysocki, and G. Gompper, Soft Matter **11**, 6680 (2015).
[49] G. Navascués and M. Berry, Mol. Phys. **34**, 649 (1977).
[50] Consider a rectangular cavity of size $L_x \times L_y$ bounded by a potential of stiffness λ_i. A direct computation leads to $\gamma = \partial \mathcal{F}/\partial L_x|_{A=L_xL_y} = -\int_{y_w}^{\infty} kT\rho(x,y)$ where x is a position in the bulk of the system and $\mathcal{F}$ the free energy [51].
[51] M. J. P. Nijmeijer and J. M. J. van Leeuwen, J. Phys. A **23**, 4211 (1990).
[52] Y. Baek, A. P. Solon, X. Xu, N. Nikola, and Y. Kafri, Phys. Rev. Lett. **120**, 058002 (2018).
[53] O. Granek, Y. Baek, Y. Kafri, and A. P. Solon, arXiv:1912.07623.
[54] W. Yan and J. F. Brady, J. Fluid Mech. **785**, R1 (2015).
[55] Y. Lanoiselée, G. Briand, O. Dauchot, and D. S. Grebenkov, Phys. Rev. E **98**, 062112 (2018).